Sains Malaysiana 52(11)(2023): 3325-3342
http://doi.org/10.17576/jsm-2023-5211-22

Elucidating the Binding Affinity of Meso Porphyrin Derivatives with Bcl-2 through Synthesis and Molecular Docking Analysis

(Elusidasi Kekuatan Ikatan Terbitan Meso Porfirin melalui Analisis Sintesis dan Pendokan Molekul)

YASOTHAA RAMAIYAH[1,2], MOHD BAKRI BAKAR[3] & MUNTAZ ABU BAKAR[1,*]

[1]Department of Chemical Sciences, Faculty of Science and Technology, Universiti Kebangsaan Malaysia, 43600 UKM Bangi, Selangor, Malaysia
[2]National Pharmaceutical Regulatory Agency, Ministry of Health Malaysia, 46200 Petaling Jaya, Selangor, Malaysia
[3]Department of Chemistry, Faculty of Science, Universiti Teknologi Malaysia, 81310 UTM Johor Bahru, Johor, Malaysia

Received: 14 September 2023/Accepted: 4 December 2023

ABSTRACT

Reversing multi-drug resistance in a clinical setting remains a formidable issue to date. Porphyrin has high efficiency to conjugate with chemotherapy drugs and effectively deliver within the nucleus of cancer cells which helps in lowering side effect to normal cells. As compared to naturally occurring beta-substituted porphyrins, synthetic meso-substituted porphyrins have numerous benefits. An extensive variety of substituents have been developed with porphyrins. There are eight new porphyrin derivatives synthesised in this research compounds **14-21** which differ from one size to another using Sonogashira and Suzuki coupling techniques. Sonogashira coupling method undergoes a reaction between alkyne terminal sp hybridized carbon and vinyl halide's sp^2 carbon in the presence of a Palladium catalyst. Furthermore, Suzuki coupling method has been an effective method in conjugation of aryl halides and borylated porphyrins. The synthesized new compounds were characterized by ultra-violet spectroscopy (UV-Vis), high resolution mass spectrometer (HRMS) and nuclear magnetic resonance (NMR) to confirm successful formation of all new compounds. The docking analysis was performed for compound **14-21.** Compounds **16** and **18** showed the greater binding mode at the Bcl-2 protein pocket regards free or metal substituted porphyrin with longer linker chain and less bulky compared to compounds **17** and **19**. This study could discover the structure of porphyrin that affects accumulation in cancer cells that potentially transmissible to target tumour.

Keywords: Bcl-2 protein; molecular docking; porphyrin; Sonogashira coupling; Suzuki coupling

ABSTRAK

Pemulihan rintangan pelbagai ubat dalam persekitaran klinikal kekal sebagai isu yang sangat kritikal setakat ini. Porfirin mempunyai kecekapan tinggi untuk bergabung dengan ubat kemoterapi dan berkesan menyampaikan ubat dalam nukleus sel kanser dan ini membantu mengurangkan kesan sampingan terhadap sel normal. Terbitan porfirin boleh diaplikasikan dalam pelbagai bidang bergantung kepada penukarganti yang diperkenalkan kepada porfirin. Berbanding dengan beta-porfirin yang wujud secara semula jadi, porfirin yang ditukarganti pada kedudukan meso secara sintetik mempunyai banyak faedah. Pelbagai jenis penukarganti porfirin telah dibangunkan. Terdapat lapan sebatian porfirin baru iaitu sebatian **14-21** yang disintesis dalam penyelidikan ini menggunakan tindak balas penggandingan Sonogashira dan Suzuki. Penggandingan Sonogashira adalah tindak balas antara karbon terhibrid terminal alkuna sp dan karbon vinil halida sp^2. Manakala, tindak balas Suzuki adalah teknik konjugasi aril halida dan porfirin terborilasi. Sebatian baharu yang disintesis telah dicirikan dengan menggunakan kaedah ultra-lembayung boleh nampak (ULBN), spektrometer jisim resolusi tinggi dan resonans magnet nuklear (RMN). Analisis dok telah dilakukan bagi sebatian **14-21**. Sebatian **16** dan **18** menunjukkan mod pengikatan yang lebih besar pada poket protein Bcl-2 iaitu sama ada bebas atau porfirin yang digantikan logam dengan rantai penghubung yang lebih panjang dan kurang besar berbanding kompaun **17** dan **19**. Kajian ini menunjukkan bagaimana struktur porfirin mempengaruhi penumpukan dalam sel kanser yang berpotensi untuk dihantar kepada tumor sasaran.

Kata kunci: Dok molekul; penggandingan Sonogashira; penggandingan Suzuki; porfirin; Protein Bcl-2

Introduction

Porphyrins are known as 'pigments of life' due to their biological potentials. Porphyrin an aromatic macrocycle made up of four pyrrole units connected by methine bridges (Park et al. 2021). The porphyrinoid cholorophyll A's absorption ability is what gives plants their green hue (Pathak et al. 2021). Porphyrins are highly beneficial due to its great absorption, emission, electron transmission and compounding characteristic because of their ring shape linked double bond properties (Fathi & Pan 2020). Porphyrins started to be synthesised in the middle of 1930s and the methods continuously been updated up to now. The rising demand for synthetic multipurpose porphyrin-based structures necessitated the discovery of new and increased efficiency to add substituents into the macrocycle and metal-catalyzed mechanisms provided this need. Symmetrical porphyrins are effortlessly synthesisable compared to unsymmetrical porphyrins (Giovannetti 2012).

Apart from photosensitizer (PS), porphyrins in photodynamic therapy (PDT) administrated though local applications or intravenously requires visible or near infrared light irradiation and oxygen present in cancer tissues are important element in destroying mitotic cells with light-dependent reaction. None of these are toxic until they systematically bonds. Selective absorption of photosensitizer into malignant cells, introduction of visible light and oxygen inactivates it. Besides of direct antitumor properties, PDT destroys cancer cell vasculature and initiates greater inflammatory which induces systemic immunity formation (Ion 2017).

Porphyrins can be directly functionalized by using organolithium reagents, which act as efficient nucleophiles to attack at the meso- and β-positions of the porphyrins. The majority of these functionalizations are carried out with different kinds of porphyrins that have reactive substituents on the porphyrin core or the substituents, such as metals, alkynes, and halogens (Gujarathi 2020). Using organolithium reagents, which effectively lithiate any meso-free position that may subsequently be substituted which developed by Senge. This is followed by an oxidative phase in an overall SNAr-type reaction. Unsubstituted porphyrin to ABCD-type porphyrin or A2B2 porphyrin to A2BC-type porphyrin could be synthesized (Nowak-krol et al. 2020).

Several coupling reactions, including the Heck, Stille, Suzuki, Sonogashira, and Buchwald-Hartwig reactions, homogeneous palladium catalysis has become extremely important in modern synthetic chemistry especially biaryl compounds or heterocyclic molecules. By using these coupling methods, several products might be synthesised either for the first time or significantly more quickly than before for the C-C bond transformations (Yin & Liebscher 2007). In 1994, the first Suzuki coupling reaction of diverse phenylboronic acids with aryl halogenides and triflates carried out by Marck, Villiger and Buchecker (1994) with Palladium/Carbon catalyst.

The Sonogashira-Hagihara reaction, which is the cross-coupling of aryl or vinyl halides (or triflate) with terminal acetylenes, was catalyzed by Pd and Cu in conjunction. Metal-catalyzed cross-coupling reactions are significant and beneficial methods for forming C-C bonds in organic synthesis (Mohjer et al. 2021). Typically, tetrahydrofuran (THF) is chosen as the preferred solvent because it increases catalytic activity and decreases susceptibility to oxygen and water (Varnado Jr. & Bielawski 2012). In this study, eight varied sizes of porphyrin derivatives were synthesised by Suzuki and Sonogashira coupling reactions. Subsequently, the synthesized porphyrin derivatives were subjected to molecular docking studies.

Breast cancer and other types of cancer in women have a terrible effect on future generations. 685,000 people died worldwide from breast cancer in 2020 which affected 2.3 million women (WHO 2023). An essential prognostic indicator for clinical breast cancer is the antiapoptosis protein known as B-cell lymphoma 2 (Bcl-2) (Eom et al. 2016). The Bcl-2 family of proteins is to set off apoptosis by closely controls permeabilization of the mitochondrial outer membrane (MOMP). Caspase activation, apoptosis, and the irreversible release of intermembrane space proteins are the results of this.

Pro-apoptogenic factors, like cytochrome c, are released into the cytosol by MOMP from the mitochondrial intermembrane space (IMS). This activates a caspase cascade that works to break up and kill the cell. The hydrophobic transmembrane motif at the C-terminus of Bcl-2-related proteins enables them to be attached to both mitochondria and the endoplasmic reticulum (ER). Bcl-2 family members regulate the exchange of Ca2+ ions effectively at the level of these interior membranes. Apoptosis which essential in growth, tissue homeostasis, and cellular stress response carried out primarily by mitochondria (Kale, Osterlund & Andrews 2018; Morris et al. 2021). Bcl-2 family members have emerged as promising targets for anticancer medications because of their diverse roles in cancer because these proteins can prevent tumour cells from dying in response to a variety of endogenous and exogenous stressors (Barillé-Nion et al. 2020).

Materials and Methods

All chemicals were analytical grade purchased from Sigma Aldrich unless otherwise stated and purified prior to use. Dichloromethane (DCM) and 1,2-Dichloroethane were dried over Phosphorus pentoxide (P_2O_5) with nitrogen gas flow for 4 h followed by a distillation process. A 3Å molecular sieve was placed in THF for 72 h before the distillation process was performed to obtain dry THF. The drying process of TEA is done by the distillation method and stored with a molecular sieve 3Å size in the dark place. Silica gel $60F_{254}$ (Merck) was used for column chromatography. Thin layer chromatography (TLC) was carried out using silica gel 60 plates (Merck). ^{1}H and ^{13}C NMR spectra were recorded on a Joel Resonance ECZ400S 400 MHz spectrometer at 400 MHz and 100 MHz, respectively, using TMS as an internal standard in $CDCl_3$ solution. Solvent residue peaks in the spectrum for the chloroform solvent used for each compound is 7.28 ppm. UV-1800 Shimadzu Spectrophotometer used to record UV-VIS spectra using dichloromethane as the solvent. High resolution mass spectrometry was carried out using a MicroTOF QIII Bruker Daltonic.

Synthesis of Dipyrromethane (DPM) 1

Paraformaldehyde (3.46 g, 120 mmol) and pyrrole (200 mL, 0.28 mmol) was added to a 3-neck round bottom flask and equipped with Schlenk technique. The solution was heated until the temperature rises to 50-70 °C and heat source was removed. Trifluoroacetic acid (TFA) (0.2 mL, 2.60 mmol) was added and a sharp increase in temperature (5-10 °C) was observed and the colour of the compound changed to black. This mixture was heated at a temperature not exceeding 90 °C for 30 min. Potassium hydroxide (KOH) (0.75 g in 25 mL H_2O) was added to stop the reaction and left at room temperature to cool. Vacuum liquid chromatography (VLC) technique is used to filter the mixture using dichloromethane solvent. The compound was concentrated with a rotary evaporator and the product purified by using Buchi 585 Kugelrohr glass oven instrument from started at 40 °C to maximum 180 °C by increasing 10 °C to produce dipyrromethane in the form of yellowish-white needle like crystals with yield of (7 g, 44 %); mp: 75 °C. The ^{13}C NMR data is identical to that reported in literature (Radzuan et al. 2018). ^{1}H NMR (400 MHz, $CDCl_3$) δ 7.76 (s, 2H), 6.63 (s, 2H), 6.15 (dd, J = 5.2 Hz, J = 2.4 Hz, 2H), 6.04 (s, 2H), 3.95 ppm (s, 2H) ppm (Scheme 1).

Synthesis of Diphenylporphyrin (DPP) 2

The synthesis of the 5,15-diphenylporphyrin compound was started with anhydrous DCM (700 mL) placed in a three round neck flask wrapped in aluminum foil along with dipyrromethene 1 (1.0 g, 6.80 mmol) and benzaldehyde (0.7 mL) with a magnetic stirrer. This product was degassed with Nitrogen gas for 10 min. Then, trifluoroacetic acid (0.1 mL) was added. This compound was allowed to stir for 18 h at room temperature. 2,3-dichloro- 5,6-dicyano-1,4-benzaquinone, DDQ (2.5 g, 11 mmol) was added after 18 h into the compound and stirred for 1 h. Triethylamine (TEA) (5 mL) was added to the compound to quench the reaction. Purification of the compound was done through the VLC technique using DCM and a rotary evaporator was used to remove the solvent. The product was left for recrystallization from DCM/Methanol (MeOH). After 96 h, the product was washed using MeOH and 5,15-diphenylporphyrin was obtained as a purple solid with yield (700 mg, 42 %); mp > 300 °C; Rf 0.5 (hexane/DCM, 3:2 v/v). The ^{13}C NMR data is identical to that reported in literature (Radzuan et al. 2018). ^{1}H NMR (400 MHz, $CDCl_3$) δ -3.10 (s, 2H), 7.80 (m, 6H), 8.27 (m, 4H), 9.07 (d, J=4.40 Hz, 4H), 9.38 (d, J=4.40 Hz, 4H), 10.30 (s, 2H) ppm (Scheme 1).

Synthesis of 5,10,15-Triphenyl Porphyrin 3

In a Schlenk flask, porphyrin (500 mg, 1.08 mmol) was added with anhydrous THF solvent (30-40 mL) under Argon atmosphere. Then, the compound was cooled to 0 °C and phenyl lithium (0.3 mL, 0.6 mmol) in 2 M cyclohexane was added dropwise over 15 min. After the compound was removed from the cold, it was stirred for another 15 min and water (0.5 mL) in THF (5 mL) was added. After stirring for 10 min (4 eq.) of DDQ was dissolved with 0.06 M DCM and the compound was stirred for another 60 min at room temperature. The mixture was filtered through silica and eluted with dichloromethane and a rotary evaporator was used to remove the solvent. The product was left for recrystallization from DCM/MeOH to yield (0.45 g, 0.84 mmol, 78 %) purple crystals; mp > 280 °C; Rf = 0.5 (3:2, hexane/DCM). The ^{13}C NMR data is identical to that reported in literature (Senge & Feng 2000). ^{1}H NMR (400 MHz, CDCl3) δ -3.10 (s, 2H), 7.80-7.81 (m, 8H), 8.26-8.29 (m, 5H), 9.08 (d, J = 4.4 Hz, 5H), 9.38(d, J = 4.8 Hz, 5H), 10.30 (s, 1H) ppm.

GENERAL PROCEDURE FOR THE SYNTHESIS OF BROMOPORPHYRINS 4-5

A 500 mL round bottom flask was filled with porphyrin (1.0 equiv.) dissolved in $CHCl_3$ solvent. Pyridine (0.6 mL) was added, and the flask immersed in ice mixed with water container to obtain a temperature of 0 °C. Then, N-bromosuccinimide (NBS) (1.0 equiv.) which had been dissolved in $CHCl_3$ solvent was added dropwise to the compound in the flask. The compound was stirred from 30 min to 1 h monitored by thin layer chromatography (TLC) technique. The mixture was filtered through silica and eluted with dichloromethane and a rotary evaporator was used to remove the solvent. The product was left for recrystallization with DCM/MeOH to yield desired product (Scheme 1).

SYNTHESIS OF 5-BROMO-10,20-DIPHENYLPORPHYRIN 4

By using 1.0 equiv. of **2** (300 mg, 0.6 mmol) and 1.0 equiv. of NBS (85 mg, 1.54 mmol) to yield **4** (0.19 g, 67 %) as violet solid; mp > 340 °C; R_f 0.5 (hexane/DCM, 3:2 v/v). The ^{13}C NMR data is identical to that reported in literature (Shanmugathasan et al. 2000). ^{1}H NMR (400 MHz, $CDCl_3$) δ -2.73 (s, 2H), 7.77-7.83 (m, 6H), 8.21-8.24 (m, 4H), 8.96-8.98 (m, 4H), 9.28 (d, *J* = 4.4 Hz, 2H), 9.75 (d, *J* = 5.2 Hz, 2H), 10.17 (s, 1H) ppm.

SYNTHESIS OF 5-BROMO-10,15,20-TRIPHENYLPORPHYRIN 5

By using 1.0 equiv. of **3** (500) mg and 1.0 equiv. of NBS to yield **5** (0.35 g, 61%) as a violet solid; mp > 300 °C. R_f 0.3 (hexane/DCM, 3:2 v/v). The ^{13}C NMR data is identical to that reported in literature (Hartnell, Edwards & Arnold 2002). ^{1}H NMR (400 MHz, $CDCl_3$) δ -3.03 (s, 2H), 7.78-7.82 (m, 12H), 8.27-8.30 (m, 3H), 9.08 (d, *J* = 5.2 Hz, 4H), 9.35 (d, *J* = 4.8 Hz, 4H).

GENERAL PROCEDURE FOR THE SYNTHESIS OF METALATED (ZINC) PORPHYRIN 6, 7, 20, 21

Porphyrin was added into a round bottom flask with $CHCl_3$ (10 mL). This compound was refluxed for 10 min. $Zn(OAc)_2$ was dissolved with Methanol and added to the porphyrin compound dropwise. The TLC technique is used to monitor after 15 min. The mixture was filtered through silica and eluted with $CHCl_3$. Purification of the product was done by crystallization technique with $CHCl_3$/MeOH solvent to obtain the desired product (Scheme 1).

SYNTHESIS OF ZINC-5,15-DIPHENYLPORPHYRIN 6

By using porphyrin **2** (50 mg, 0.1 mmol) to yield **6** (56 mg, 99%); mp: 360 °C; Rf (hexane: $CHCl_3$, 1:1): 0.6. The ^{13}C NMR data is identical to that reported in literature (Mohd Radzuan et al. 2021). NMR ^{1}H (400 MHz, $CDCl_3$) δ: 7.80-7.84 (m, 6H), 8.28-8.31 (m, 4H), 9.16 (d, *J* = 4.8 Hz, 4H), 9.46 (d, *J* = 4.8 Hz, 4H), 10.35 (s, 2H) ppm.

SYNTHESIS OF ZINC-5,10,15-TRIPHENYLPORPHYRIN 7

By using porphyrin **3** (50 mg, 0.1 mmol) to yield **7** (54 mg, 97%); mp: 360 °C; Rf (hexane: $CHCl_3$, 1:1) 0.6. The ^{13}C NMR data is identical to that reported in literature (Locos & Arnold 2006). NMR ^{1}H (400 MHz, $CDCl_3$) δ: 7.78-7.82 (m, 9H), 8.24-8.29 (m, 6H), 9.15 (d, *J* = 4.8 Hz, 4H), 9.45 (d, *J* = 4.8 Hz, 4H), 10.34 (s, 1H) ppm.

SYNTHESIS OF ZINC-5-(PHENYL ACETYL)-10,20-DIPHENYLPORPHYRIN 20

By using **14** (80 mg) to yield **20** as purple crystals (60 mg, 54%) mp: 360 °C; Rf (hexane: $CHCl_3$, 1:1): 0.6; NMR ^{1}H (400 MHz $CDCl_3$) δ: 0.05 (s, 1H), 7.75-7.77 (m, 10H), 8.20-8.23 (m, 6H), 9.09 (d, *J* = 4.4 Hz, 4H), 9.38 (d, *J* = 4.4 Hz, 4H), 10.28 (s, 1H) ppm. ^{13}C NMR (100.6 MHz, $CDCl_3$): δ 1.01, 10.95, 14.02, 22.97, 23.76, 24.57, 28.93, 29.69, 30.37, 38.75, 68.16, 126.62, 126.97, 127.70, 128.80, 130.87, 131.03, 131.60, 131.70, 132.48, 134.64, 134.84, 206.92 ppm. HRMS calculated for $C_{40}H_{26}N_4OZn$: 644.06, found 644.28.

SYNTHESIS OF ZINC-5-(PHENYL ACETYL)-10,15,20-TRIPHENYLPORPHYRIN 21

By using **15** (100 mg) to yield **21** as purple crystals (75 mg, 68%). mp: 360 °C; Rf (hexane: $CHCl_3$, 1:1): 0.6; NMR ^{1}H (400 MHz, $CDCl_3$) δ: 0.07 (s, 1H), 7.75-7.81 (m, 12H), 8.22-8.27 (m, 6H), 9.12 (d, *J* = 4.4 Hz, 4H), 9.41 (d, *J* = 4.4 Hz, 4H) ppm. ^{13}C NMR (100.6 MHz, CDCl3): δ 1.02, 10.97, 14.04, 22.99, 23.77, 24.58, 28.95, 29.75, 30.39, 34.72, 38.76, 44,12, 106.24, 119.13, 126.66, 126.99, 130.88, 131.75, 132.53, 134.66, 134.87, 149.50, 150.16 ppm. HRMS calculated for $C_{46}H_{30}N_4OZn$: 718.17, found: 718.49.

GENERAL PROCEDURE FOR THE SYNTHESIS OF BORYLATED PORPHYRINS 8-9

Porphyrin-boronate was synthesized using the method of Dahms et al. Bromoporphyrin (222.70 g, 0.36 mmol) and catalyst $PdCl_2$ $(PPh_3)_2$ were placed in a round bottom

flask and the moisture removed using vacuum suction. 1,2-dichloroethane anhydrous solvent (23.0 mL) and triethylamine (TEA) anhydrous solvent (0.7 mL, 4.69 mmol) added into the bromoporphyrin compound. Three times the freeze-pump-thaw technique is performed to ensure an inert state (Schlenk technique) achieved. Then, pinacolborane (1.1 mL, 7.20 mmol) was added and stirred at 75 °C for 45 min. The TLC technique is used to monitor the reaction quenced after all the starting materials have reacted. Mixture filtered using vacuum liquid chromatography with hexane:DCM = 1:1 v/v). Purification of the product was done by crystallization technique with $CHCl_3$/MeOH (Scheme 1).

SYNTHESIS OF 5-(4,4,5,5-TETRAMETHYL-1,3,2-DIOXABOROLANE) 10,20-DIPHENYLPORPHYRIN 8

By using **4** (126 mg) to yield **10** as a violet colour crystal (85 mg, 66 %); mp >350 °C. R_f 0.3 (hexane/DCM, 1:1, v/v). The ^{13}C NMR data is identical to that reported in literature (Bakar et al. 2011). ^{1}H NMR (400 MHz, $CDCl_3$) δ -3.08 (s, 2H), 2.18 (s, 12H), 7.82-7.83 (m, 6H), 8.28-8.30 (m, 4H), 9.10 (d, *J* = 4.4 Hz, 4H), 9.41 (d, 4H), 10.33 (s, 1H) ppm.

SYNTHESIS OF 5-(4,4,5,5-TETRAMETHYL-1,3,2-DIOXABOROLANE)-10,15,20-TRIPHENYLPORPHYRIN 9

By using **5** (318.68 mg) to yield **11** as a violet colour crystal (290 mg, 84%); mp: 360 °C. R_f 0.3 (hexane/DCM, 1:1, v/v). The ^{13}C NMR data is identical to that reported in literature (Bakar et al. 2011). ^{1}H NMR (400 MHz, $CDCl_3$) δ -3.10 (s, 2H), 1.85 (s, 12H), 7.80-7.82 (m, 9H), 8.24-8.30 (m, 6H), 9.09 (d, *J* = 4.4 Hz, 4H), 9.40 (d, *J* = 4.8 Hz, 4H) ppm.

GENERAL PROCEDURE FOR THE SYNTHESIS OF LINKER CONJUGATED PORPHYRIN VIA SUZUKI COUPLING REACTION 14-15

A heterogeneous solution of borylated porphyrin (0.14 mmol), phenyl acetyl chloride (1.0 equivalent), Cs_2CO_3 (2.0 equiv.) and $Pd(PPh_3)_4$ (0.13 equiv,) in THF (20 mL) was refluxed under argon at 77 °C for 24-48 h (monitored by TLC). The reaction mixture was filtered through silica gel and washed with DCM. After removal of the solvent under reduced pressure the residue was chromatographed on silica gel (hexane:DCM, 1:1, v/v) and recrystallized with DCM/MeOH (Scheme 1).

SYNTHESIS OF 5-(PHENYL ACETYL)-10,20-DIPHENYLPORPHYRIN 14

By using **8** (100 mg) to yield **14** as purple crystals (65 mg, 66%). ^{1}H NMR (400 MHz, $CDCl_3$) δ -3.10 (s, 2H), 0.09 (s, 1H), 7.80-7.82 (m, 10H), 8.27-8.29 (m, 6H), 9.08 (d, *J* = 4.4 Hz, 4H), 9.38 (d, *J* = 4.8 Hz, 4H), 10.30 (s, 1H) ppm. ^{13}C NMR (100.6 MHz, $CDCl_3$): δ 1.07, 9.61, 29.74, 99.10, 105.29, 119.14, 126.77, 127.00, 127.75, 131.07, 131.63, 134.64, 134.88, 141.43, 145.24, 147.22, 159.12 ppm. HRMS calculated for $C_{40}H_{28}N_4O$ $[M+H]^+$: 580.23, found: 594.72.

SYNTHESIS OF 5-(PHENYL ACETYL)-10,15,20-TRIPHENYLPORPHYRIN 15

By using **9** (100 mg) to yield **15** as purple crystals (55 mg, 56%). ^{1}H NMR (400 MHz, $CDCl_3$) δ -3.09 (s, 2H), 0.10 (s, 1H), 7.79-7.83 (m, 12H), 8.28-8.30 (m, 6H), 9.09 (d, *J* = 4.4 Hz, 4H), 9.40 (d, *J* = 4.4 Hz, 4H) ppm. ^{13}C NMR (100.6 MHz, $CDCl_3$): δ 1.04, 10.99, 14.07, 23.01, 23.80, 28.97, 30.41, 38.78, 68.20, 99.21, 105.28, 119.13, 126.77, 126.99, 127.74, 128.43, 128.58, 128.83, 130.89, 131.07, 131.62, 132.51, 134.63, 134.87 ppm. HRMS calculated for $C_{46}H_{32}N_4O$ $[M+H]^+$: 656.26, found: 670.82.

GENERAL PROCEDURE TO SYNTHESIS OF FREE BASE AND METAL PORPHYRIN DERIVATIVES SUBSTITUTED WITH ETHYNYL PHENYL 10-13

Mono ethynylphenyl substitutions in pophyrins have been synthesized on a large scale via organolithium reactions starting from commercially available 1-bromo-4-ethynylbenzene. The reaction was carried out with an excess of n-BuLi followed by the addition of porphyrin (1.0 equivalents) in THF. Column chromatography was performed using neutral alumina and hexane: DCM 1:1 (v/v) as solvent.

SYNTHESIS OF 5-(4-ETHYNYL-PHENYL)-10,20-DIPHENYLPORPHYRIN 10

1-Bromo-4-ethynylbenzene (0.50 g, 2.76 mmol) was dissolved in anhydrous diethylether (10 mL) in a 250 mL Schlenk tube. n-BuLi (2.2 mL, 5.52 mmol in a 2.5 hexane solution) was added dropwise over 30 min under argon at -70 °C. The compound was stirred until the temperature reached -40 °C and THF (2 mL) was added dropwise until the aryl lithium compound formed a white (light pink to white) suspension. After

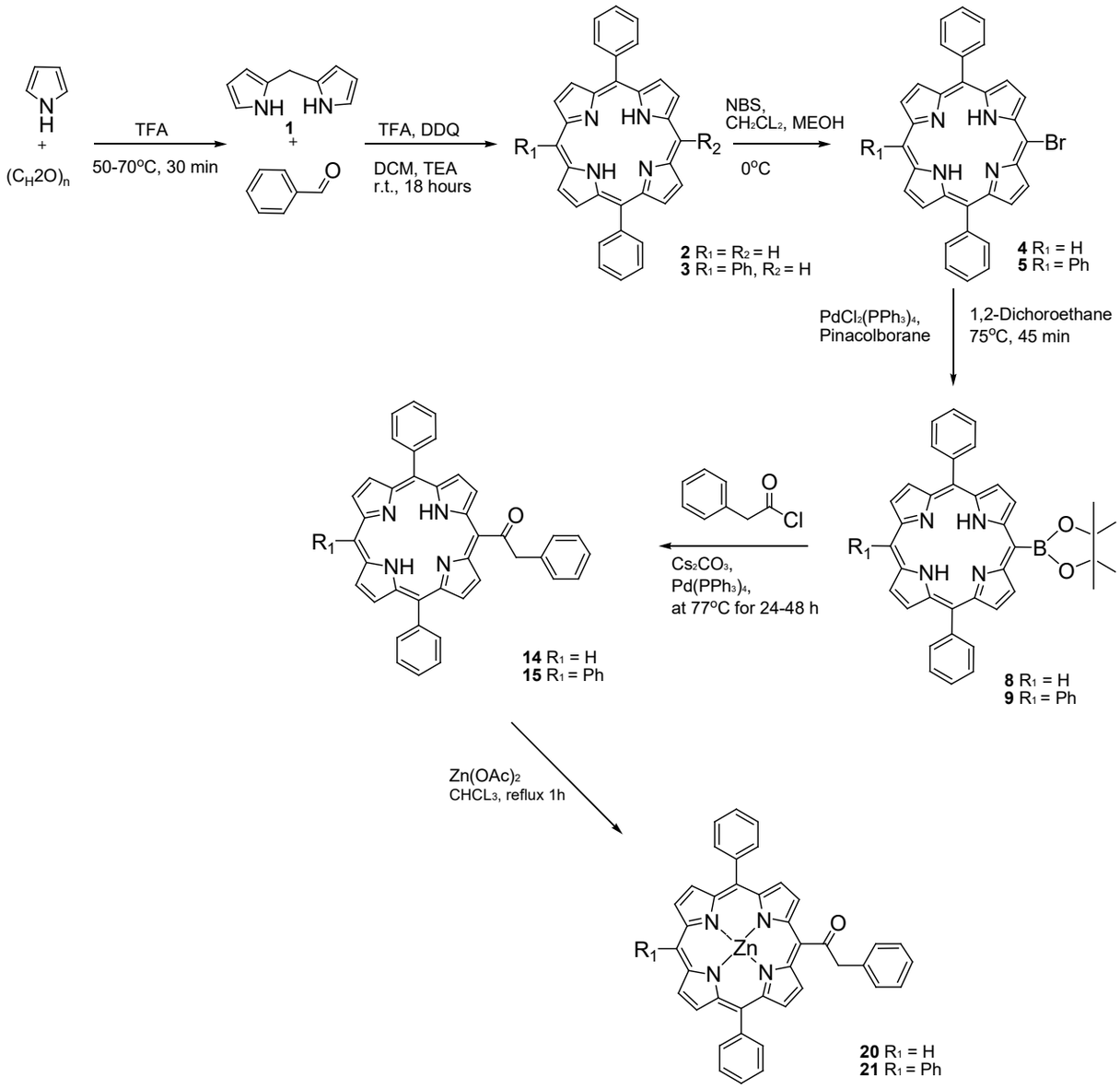

SCHEME 1. Synthesis of compounds 1-5, 8, 9, 14, 15. 20 and 21

ice removal, the mixture was stirred for 15 min under argon. 5,15-diphenylporphyrin (100 mg, 0.19 mmol) in anhydrous THF (50 mL) was cooled to 0 °C and then added under argon to the vigorously stirred reaction mixture. The ice water was removed, and the mixture was stirred for 1 h (monitored by TLC), followed by the addition of saturated NH_4Cl (1 mL) and stirring for 30 min. 10.0 equivalents of DDQ (0.06 M THF) was added. After 1 h, the reaction mixture was filtered through neutral alumina, with DCM. Column chromatography was performed using neutral alumina and hexane: DCM 20:1 (v/v) as solvent to yield **10** as a violet colour crystal (65 mg, 53%); mp >300 °C. R_f 0.3 (hexane/DCM, 1:1, v/v). The ^{13}C NMR data is identical to that reported in

literature (Feng & Senge 2001). ^{1}H NMR (400 MHz, $CDCl_3$) δ -3.09 (s, 2H), 3.50 (s, 1H), 7.80-7.82 (m, 8H), 8.29 (d, *J* = 3.2 Hz, 4H), 9.08 (d, *J* = 4.4 Hz, 4H), 9.40 (d, *J* = 4.4 Hz, 4H), 10.33 (s, 1H) ppm (Scheme 2).

SYNTHESIS OF 5-(4-ETHYNYL-PHENYL)-10,15,20-TRIPHENYLPORPHYRIN 11

By using **3** (100 mg) to yield **11** as purple crystals (60 mg, 51%). The ^{13}C NMR data is identical to that reported in literature (Ryan et al. 2011). ^{1}H NMR (400 MHz, $CDCl_3$) δ -3.09 (s, 2H), 3.50 (s, 1H), 7.82-7.83 (m, 12H), 8.28-8.30 (m, 7H), 9.10 (d, *J* = 4.4 Hz, 4H), 9.41 (d, *J* = 4.8 Hz, 4H).

SYNTHESIS OF ZINC-5-(4-ETHYNYL-PHENYL)-10,20-DIPHENYLPORPHYRIN 12

By using **6** (100 mg) to yield **16** as purple crystals (65 mg, 55%). The ^{13}C NMR data is identical to that reported in literature (Ryan et al. 2011). ^{1}H NMR (400 MHz, $CDCl_3$) δ 3.33 (s, 1H), 7.76-7.80 (m, 9H), 8.25-8.27 (m, 5H), 9.13 (d, *J* = 4.8 Hz, 4H), 9.43 (d, *J* = 4.4 Hz, 4H), 10.31(s, 1H).

SYNTHESIS OF ZINC-5-(4-ETHYNYL-PHENYL)-10,15,20-TRIPHENYLPORPHYRIN 13

By using **7** (100 mg) to yield **17** as purple crystals (75 mg, 64%). The ^{13}C NMR data is identical to that reported in literature (Nakano et al. 2001). ^{1}H NMR (400 MHz, $CDCl_3$) δ 3.33 (s, 1H), 7.76-7.80 (m, 11H), 8.24-8.27 (m, 8H), 9.13 (d, *J* = 4.8 Hz, 4H), 9.43 (d, *J* = 4.4 Hz, 4H).

GENERAL PROCEDURE FOR THE SYNTHESIS OF LINKER CONJUGATED PORPHYRIN VIA SONOGASHIRA COUPLING REACTION 16-19

Brominated porphyrin in the presence of $PdCl_2(PPh_3)_2$ as a catalyst in THF was used in this coupling. A heterogeneous solution of ethyl substituted porphyrin (1.0 equivalent) and phenyl acetyl chloride (1.0 equivalent) with anhydrous THF (15 mL and anhydrous TEA (5 mL) was added to a 50 mL Schlenk tube. The mixture is degassed (freeze-pump-thaw) three times followed by the addition of CuI (0.2 equivalent) and the mixture is degassed again. $PdCl_2(PPh_3)_2$ (0.1 equivalent) was added, and the mixture was refluxed under argon at 60 °C in a closed system for 24-48 h (monitored by TLC). The reaction mixture was filtered through silica gel and washed with DCM. After removal of solvent, chromatography on silica gel (hexane/DCM 3:2 v/v) and recrystallization from DCM/MeOH (Scheme 2).

SYNTHESIS OF 5,15-DIPHENYL-20-{4-[(PHENYLACETYL) ETHYNYL] PHENYL} PORPHYRIN 16

By using **10** (100 mg) to yield **16** as purple crystals (70 mg, 58%) ^{1}H NMR (400 MHz, $CDCl_3$) δ -3.09 (s, 2H), 0.08 (s, 1H), 7.80-7.82 (m, 12H), 8.27-8.29 (m, 8H), 9.08 (d, *J* = 4.4 Hz, 4H), 9.39 (d, *J* = 4.8 Hz, 4H), 10.32 (s, 1H) ppm. ^{13}C NMR (100.6 MHz, $CDCl_3$): δ 0.54, 1.024, 10.48, 29.71, 33.16, 49.11, 51.06, 74.85, 97.25, 103.00, 126.41, 127.07, 128.36, 128.73, 129.02, 129.51, 129.79, 131.07, 131.10, 131.64, 131.99, 132.16, 138.54, 165.14 ppm. HRMS calculated $C_{48}H_{32}N_4O$: 680.26, found 681.81.

SYNTHESIS OF 5,10,15-TRIPHENYL-20-{4-[(PHENYLACETYL)ETHYNYL] PHENYL} PORPHYRIN 17

By using **11** (100 mg) to yield **17** as purple crystals (65 mg, 55%). ^{1}H NMR (400 MHz, $CDCl_3$) δ -3.08 (s, 2H), 0.07 (s, 1H), 7.53-8.28 (m, 25H), 9.08 (s, 3H), 9.37(d, *J* = 20 Hz, 4H), 10.32 (s, 1H) ppm. ^{13}C NMR (100.6 MHz, $CDCl_3$): δ 1.02, 1.04, 20.56, 29.70, 38.76, 69.57, 99.56, 106.57, 126.41, 128.37, 128.48, 128.61, 129.80, 132.10, 132.19, 143.32, 145.73, 146.46, 174.96, 181.57, 213.75 ppm. HRMS calculated $C_{54}H_{36}N_4O$: 756.29, found: 756.72.

SYNTHESIS OF ZINC-5,15-DIPHENYL-20-{4-[(PHENYLACETYL)ETHYNYL] PHENYL} PORPHYRIN 18

By using **12** (100 mg) to yield **18** as purple crystals (62 mg, 52%). ^{1}H NMR (400 MHz, $CDCl_3$) δ 0.08 (s, 1H), 7.78-7.82 (m, 12H), 8.27-8.30 (m, 8H), 9.16 (d, *J* = 4.4 Hz, 4H), 9.45 (d, *J* = 4.4 Hz, 4H), 10.34 (s, 1H) ppm. ^{13}C NMR (100.6 MHz, $CDCl_3$): δ 0.10, 1.02, 20.67, 29.70, 44.56, 45.73, 52.85, 57.78, 59.34, 69.26, 88.54, 99.10, 126.66, 127.00, 127.22, 127.52, 130.61, 131.62, 131.77, 132.55, 134.29, 134.65, 134.88, 143.18, 149.53, 150.18, 160.88, 178.23, 183.23, 186.87, 191.90, 192. 55, 196.24, 198.32, 206.90, 210.64, 214.82 ppm. HRMS calculated $C_{48}H_{30}N_4OZn$ $[M+H]^{+}$: 742.17, found: 756.19.

SYNTHESIS OF ZN-5,10,15-TRIPHENYL-20-{4-[(PHENYLACETYL)ETHYNYL] PHENYL} PORPHYRIN 19

By using **13** (100 mg) to yield **19** as purple crystals (76 mg, 65%). ^{1}H NMR (400 MHz, $CDCl_3$) δ 0.07 (s, 1H), 7.53-8.27 (m, 25H), 9.14 (d, *J* = 4.4 Hz, 3H), 9.43(d, *J* = 4.4 Hz, 4H), 10.32 (s, 1H) ppm. ^{13}C NMR (100.6 MHz, $CDCl_3$): δ 0.29, 0.65, 0.72, 1.02, 1.39, 1.81, 14.11, 14.88, 29.36, 29.70, 30.16, 30.56, 30.93, 31.93, 43.61, 58.68, 65.90, 70.75, 87.32, 91.32, 100.00, 112.26, 126.41,

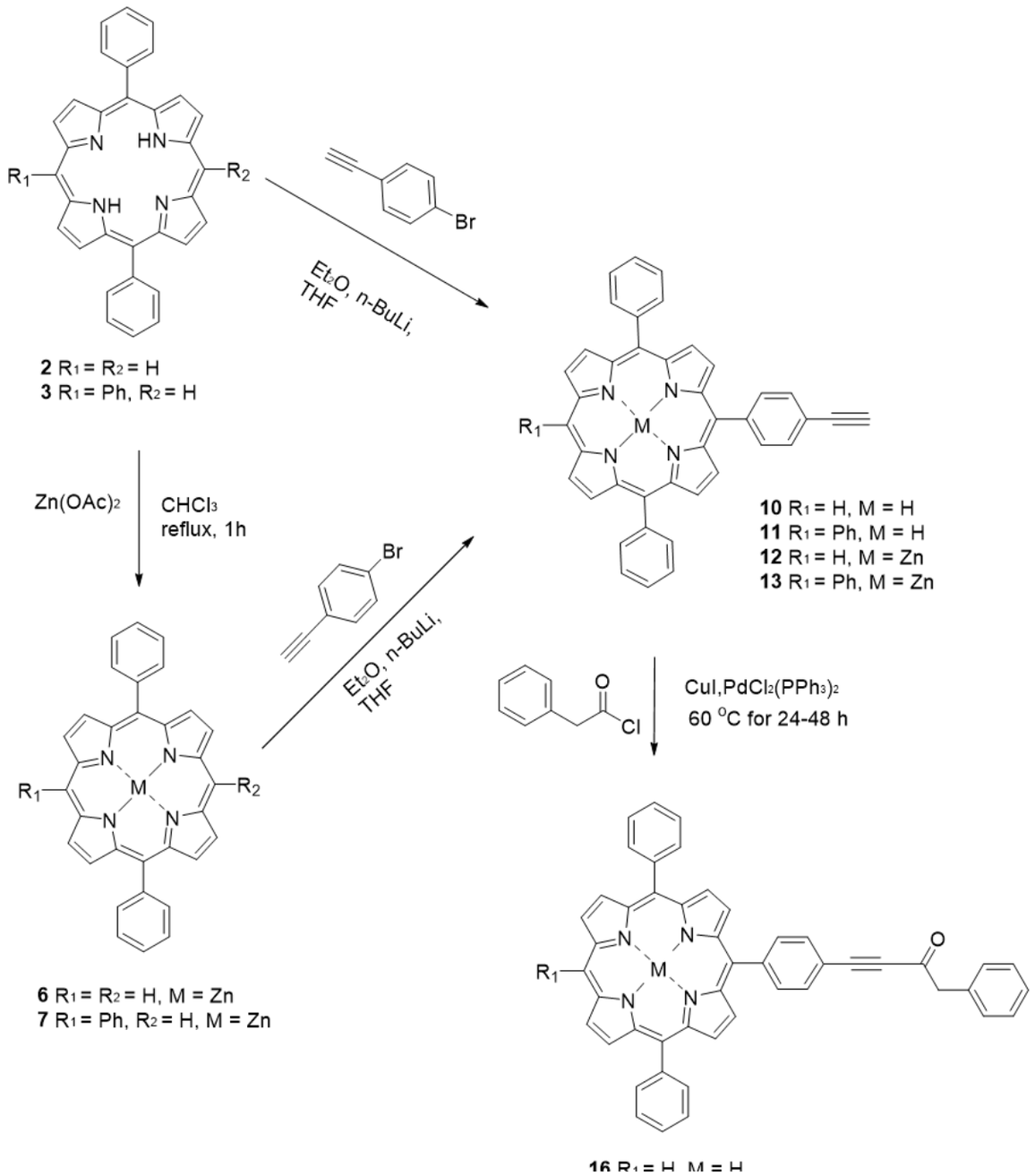

SCHEME 2. Synthesis of compounds 6, 7, 10-13 and 16-19

127.10, 131.75, 161.24, 162.68, 163.12, 163.90, 165.86, 167.88, 183.89, 184.23, 185.21, 191.39, 204.24, 213.83 ppm. HRMS calculated $C_{54}H_{34}N_4OZn$: 818.20, found: 818.56.

DOCKING STUDIES

In the beginning, eight compounds were drawn and set up for geometry optimization. All the ligand molecules were optimized at the DFT-B3LYP/6-31G(d) level using

Gaussian 09 program (Saini et al. 2019). To calculate the electrostatic potential (ESP) atomic charges (Rathi, Ludlow & Verdonk 2020) for the ligands in the molecular docking simulation, the keyword POP=ESP was included in the Gaussian put files (.com). On the other side, the crystal structure of the receptor, (PDB ID: 4LVT) (Phan et al. 2005) was extracted from the Protein Data Bank website (https://www.rcsb.org/). The ligand and water molecules were removed and the pure receptor (4LVT) was employed for the energy minimization by OPLS-AA force field (Monvall 1976) using Gromacs version 2021 (Van Der Spoel et al. 2005). AutoDock Tools (ADT) 4.2 was used for preparing the receptor-ligand complex systems. All the polar hydrogens were added by using the Hydrogen module and Gasteiger partial charges (Gasteiger & Marsili 1980; Han & Zhang 2010) were assigned for the receptor. Molecular docking of the eight compounds to the (4LVT) model was carried out using AutoDock software package. The tools available in the package including AutoDock Vina 1.1.2 (Allouche 2012). The AutoDock Vina tool uses a united atom scoring functions and allows finding the best binding pocket in receptors for ligand molecules. A grid size of 80 × 80 × 80 points with a spacing of 0.503 Å was applied which covered whole the receptor structure. At the end, all the interactions between 4LVT receptor and eight compounds were analysed by discovery studio (DS).

Results and Discussions

This work reports the synthesis of new porphyrin derivatives by Sonogashira coupling **16-19** (Scheme 2) method and Suzuki-Miyaura coupling **14, 15, 20** and **21** (Scheme 1) which were evaluated for molecular docking to obtain greater binding affinity compound on Bcl-2. Under nitrogen purging conditions, the light-sensitive and less stable dipyrromethene **1** was synthesised, and needle like yellowish crystal was produced by heating in vacuum using a Kugelrohr glass oven at 160-180 °C to obtain highly purified dipyrromethene **1**. The privilege of synthesis porphyrin with dipyrromethane as starting compound is to avoid mixing of undesired porphyrin byproducts. The 5,15-diphenylporphyrin **2** with two free meso positioned symmetric porphyrin were chosen as starting material as they are efficiently synthesized in one step reaction and greater yields from dipyrromethene and benzaldehyde. This is important because of organolithium reagents and halogen to be substituted without substituting into β positions of the porphyrin.

The porphyrin **3** (A_3B) with phenyl substitution, porphyrin **10-13** with ethynylbenzene substitution were synthesized by the reaction of organolithium reagents such as phenyl lithium and n-BuLi with porphyrin **2**. Halogenated (Br) porphyrin synthesised with 1.0 equiv. of NBS to obtain compounds **4** and **5**. This procedure was conducted in a cooled (0 °C) solution to avoid lack of selectivity and difficulty for liquid chromatographic separation of the mono- and dibrominated compounds.

Borylated porphyrins **8** and **9** were synthesized from bromoporphyrins **4** and **5** via Pd-catalyzed reaction with 4,4,5,5-tetramethyl-1,3,2-dioxaborolane. The reactions were conducted by employing an excess of pinacolborane with the brominated porphyrin, leading to yields of **8-9** at 66% and 84%, respectively. These outcomes showed a favourable binding site capable of potentially interacting with prodrug linkers. The Suzuki coupling reaction, which uses the cross-coupling of organoboron reagents with phenyl acetyl chloride using Pd-catalyzed carbon-carbon bond synthesis strategies to obtain compounds **14-15.** Longer linker conjugated porphyrin **16-19** synthesised with Sonogashira coupling method. The alkyne-linked porphyrin **10-13** was synthesised through palladium catalyzed reaction with 1-Bromo-4-ethynylbenzene in 53%, 51%, 55% and 64% respectively. Sonogashira reaction was succesfully carried out with phosphine base palladium catalyst that is $PdCl_2(PPh_3)_2$ and CuI as a co-catalyst in TEA solvent.

The typical absorption spectrum of porphyrins includes a strong band (Soret band) in the 400-440 nm range and four weaker Q bands (Qy(1,0), Qy (0,0), Qx (1,0), and Qx (0,0)) in the 440-800 nm range (Boscencu et al. 2023). The distinct properties of the metal ions and the substituents on the ring have an impact on the relative intensity that provide changes to the bands of absorption in porphyrin complexes (Giovannetti 2012). The number of Q bands reduces as the symmetry of the molecule rises when the metal ion coordinates with the nitrogen atoms (Zheng et al. 2008). Table 1 shows the absorption data (soret band and Q band) of new porphyrin derivatives synthesised in this research.

The absorption spectra of the metal-free porphyrins **14-17** showed an ordinary Soret band and four Q bands of porphyrin compounds. Moreover, spectra shows that variation in the peripheral substituents indicates no change to the UV-VIS results for the free-base porphyrins. Table 1 shows close similarity absorption data for the compounds **14-17**. Soret band was assigned

in the range of 400 to 410 nm. Besides that, four absorption maxima attributed in the Q band in all free base porphyrin. A metal ion connected to a pyrrole ring occupies the center of the metalloporphyrin ring. The metal ion takes the lone-pair electrons of the N atoms in the pyrrole rings, and metal ion electrons are donated to the porphyrin molecule to form delocalized π bonds that allow the electrons in the delocalized system to flow easily. Metalloporphyrin (**18-21)** indicate two absorption peaks on Q band. This shows delocalized π bands of the Zn(II) substituted porphyrin elevates the porphyrin's average electron density, which reduces the energy for electron transition.

DOCKING STUDIES

Computer-assisted drug design frequently use molecular docking to foretell the preferred orientation and binding affinities of the drug-protein complexes. To investigate the most active porphyrin derivatives and molecular target Bcl-2, they have been docked into the binding active site of the anti-apoptotic protein Bcl-2 (code: 4LVT). Binding location and orientation of porphyrin derivatives on 4LVT as predicted by the Autodock Vina 1.1.2 software. Active residues interacting with each ligand via electrostatic π-cation, hydrogen bond π-Donor, hydrophobic π- π stacked, hydrophobic π- π t shaped and hydrophobic π-Alkyl. When the stabilizing energy is negative, the ligand attaches on its own without using any energy. The average binding energies between the 4LVT protein with compounds **14, 15, 16, 17, 18, 19, 20, 21** were found to be -11.3 kcal/mol, -10.9 kcal/mol, -11.3 kcal/mol, -11.0 kcal/mol, -9.7 kcal/mol, -9.6 kcal/mol, -9.7 kcal/mol, and -9.6 kcal/mol, respectively. Compounds **16** and **18** seem to have better affinities to 4LVT. Figures 1-8 show the interaction of each porphyrin derivative **14** -**21** of 2D and 3D orientation with active pocket of 4LVT.

Binding pocket of the 4LVT formed intermolecular interactions with compounds target by conserved amino acid residues of ARG143, ASN140, TYR105, PHE101, MET112, PHE195, ALA146, VAL145, and ALA97. Hydrogen bond pi-donor of ASN140-ligand observed in compounds **16-19**. The absence of a substituted ethynyl phenylbenzene moiety was not discerned within the structural composition of the remaining compound. The hydrophobic interactions observed in the porphyrin derivatives were predominantly constituted by π-π stacking, π-π T-shaped stacking, and π -alkyl interactions. Hydrophobic π-π stacked took place between ligand-TYR105 in all docked compounds. PHE101 and TYR105 π-π T-shaped hydrophobic were detected in **16-19.** Whilst PHE101, TYR105, and PHE195 interaction between ligands observed in pi-pi T-shaped hydrophobic in rest of the compounds. Meanwhile, compounds **16-19** established four hydrophobic π-alkyl type of interaction that is, ARG143, ALA146, MET112, and ALA97. VAL145 interaction site additionally been observed in compounds **14-15** and **20-21** as hydrophobic π-alkyl apart from ALA97, ARG143, and ALA146. Furthermore, electrostatic π-cation with ARG143-ligand binding tool place in compounds **16-19** as shown in Table 2.

TABLE 1. Absorption data in DCM (soret band and Q band) of new porphyrin derivatives **14-19**

Compounds	Soret band λ (nm)	Q band λ (nm)
14	410	502, 528, 574, 630
15	400	507, 537, 580, 635
20	406	536, 574
21	400	535, 569
16	410	507, 541, 581, 632
17	404	507, 542, 584, 634

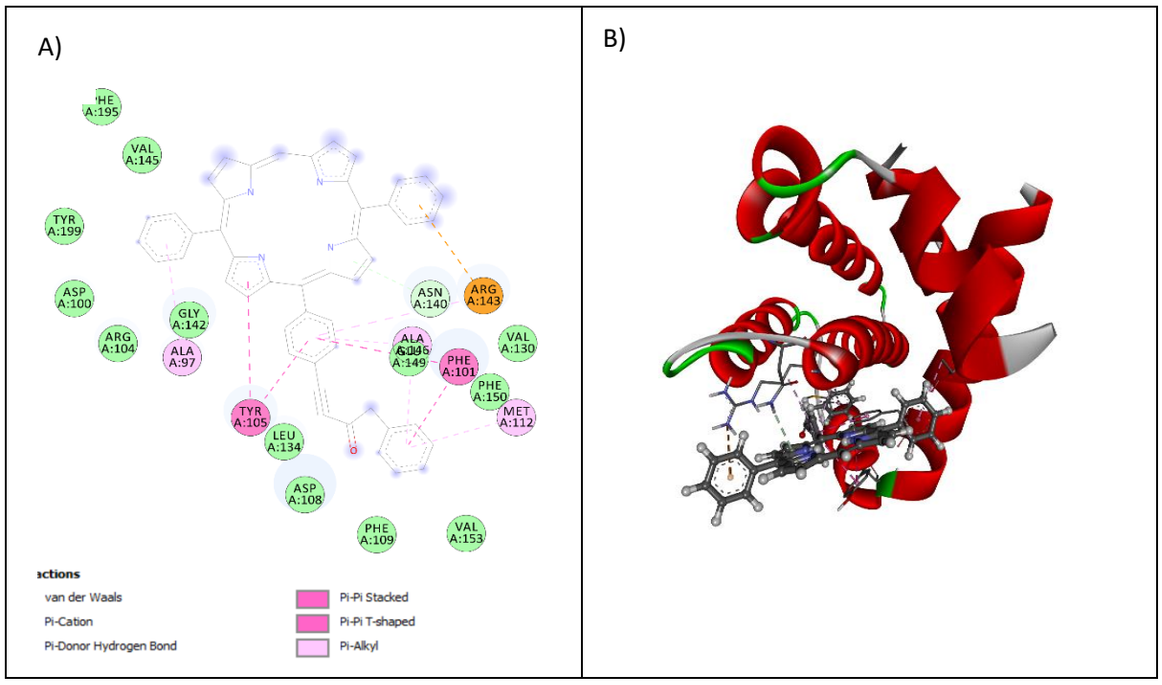

FIGURE 1. A) 2D orientation of the docked compound **16** in the active pocket of 4LVT.
B) 3D– Putative docking interaction of ligand **16** that was in complex of 4LVT

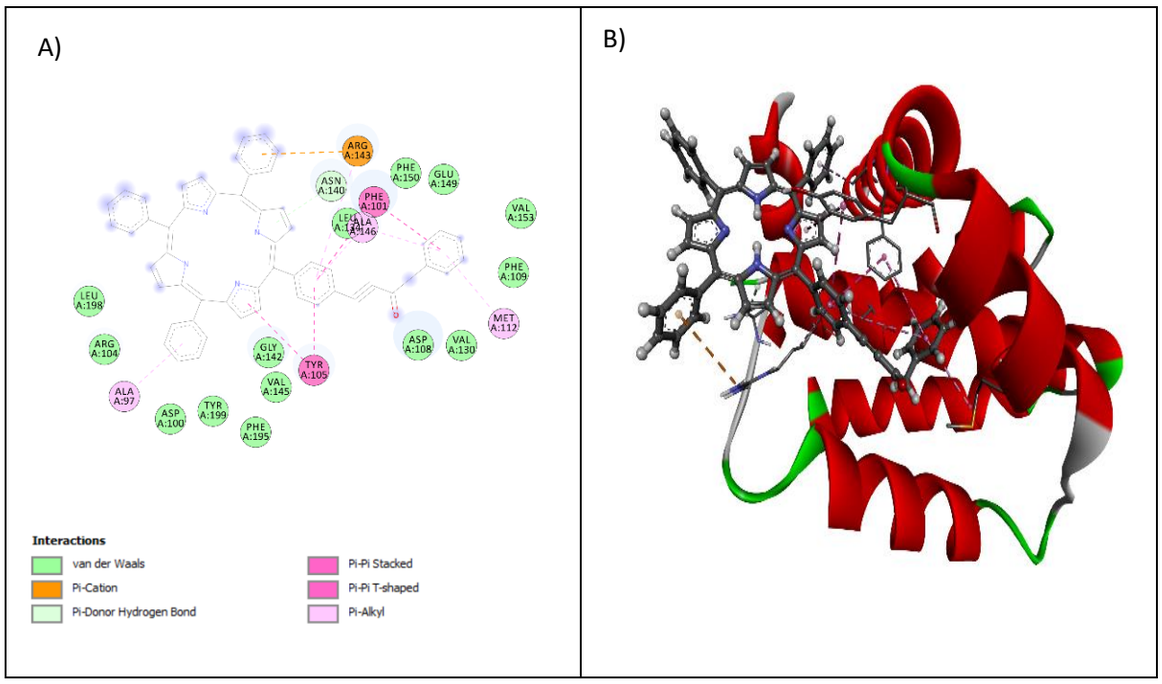

FIGURE 2. A) 2D orientation of the docked compound **17** in the active pocket of 4LVT.
B) 3D– Putative docking interaction of ligand **17** that was in complex of 4LVT

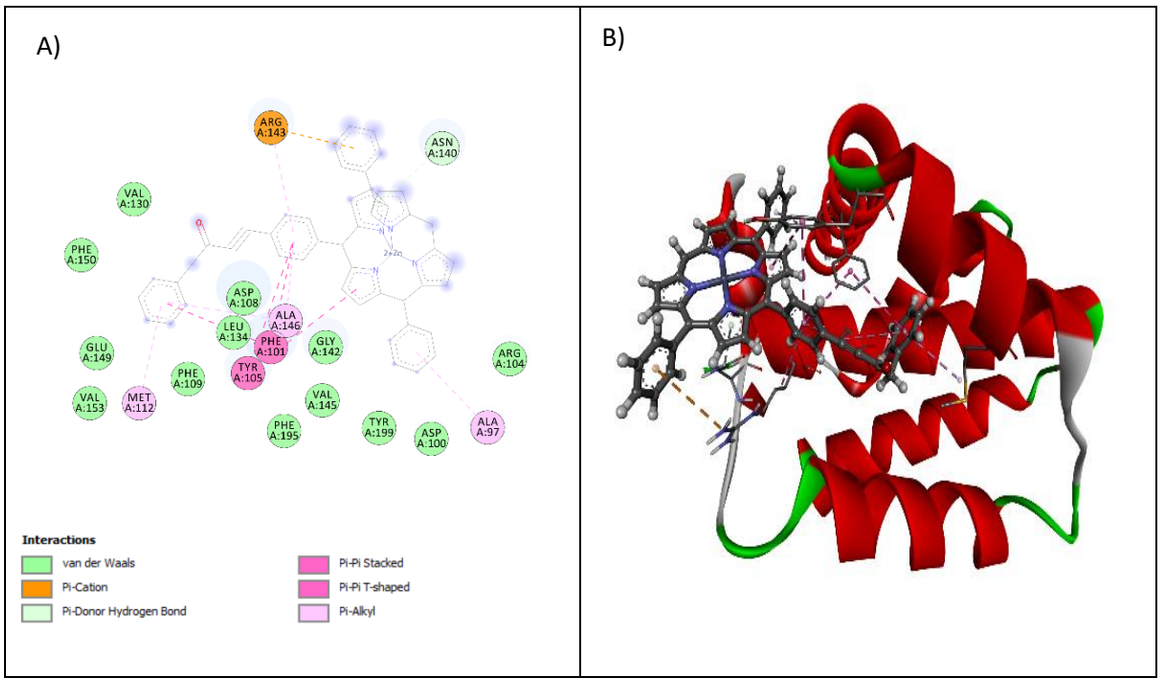

FIGURE 3. A) 2D orientation of the docked compound **18** in the active pocket of 4LVT.
B) 3D– Putative docking interaction of ligand **18** that was in complex of 4LVT

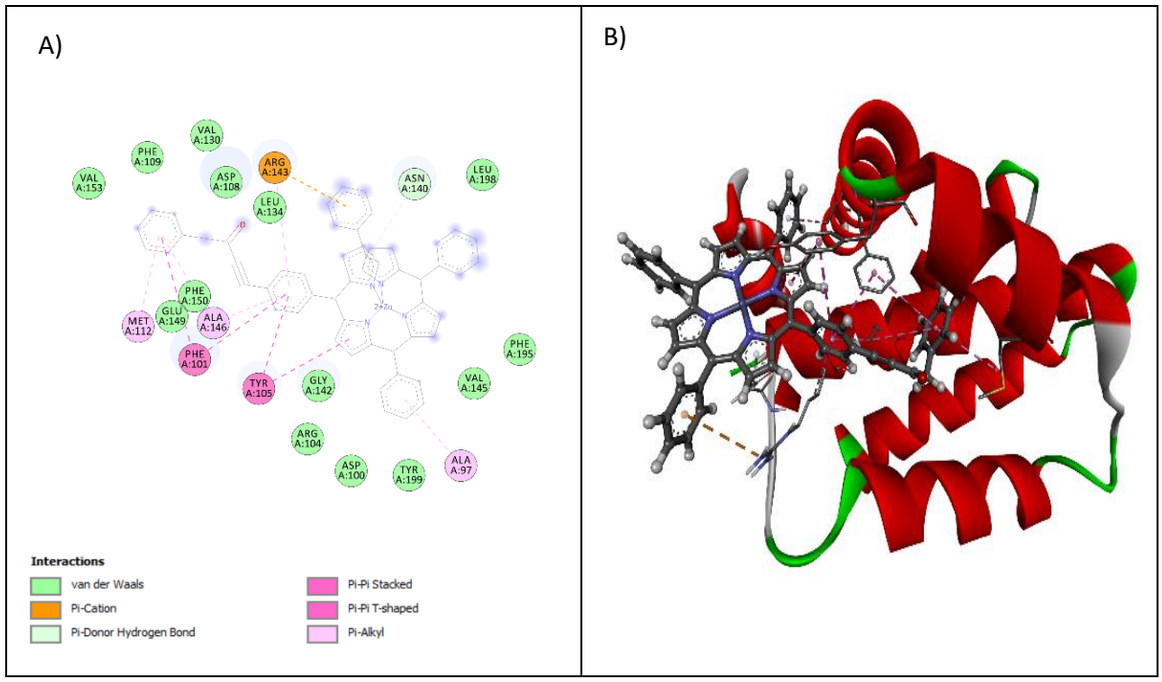

FIGURE 4. A) 2D orientation of the docked compound **19** in the active pocket of 4LVT.
B) 3D– Putative docking interaction of ligand **19** that was in complex of 4LVT

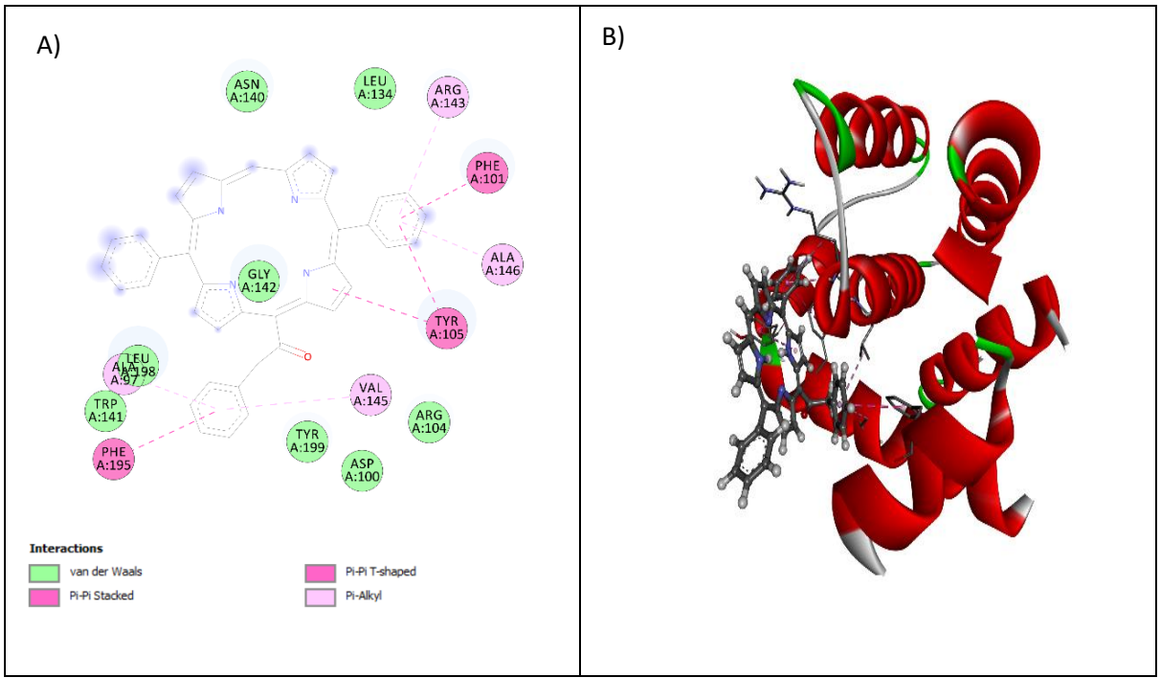

FIGURE 5. A) 2D orientation of the docked compound **14** in the active pocket of 4LVT.
B) 3D– Putative docking interaction of ligand **14** that was in complex of 4LVT

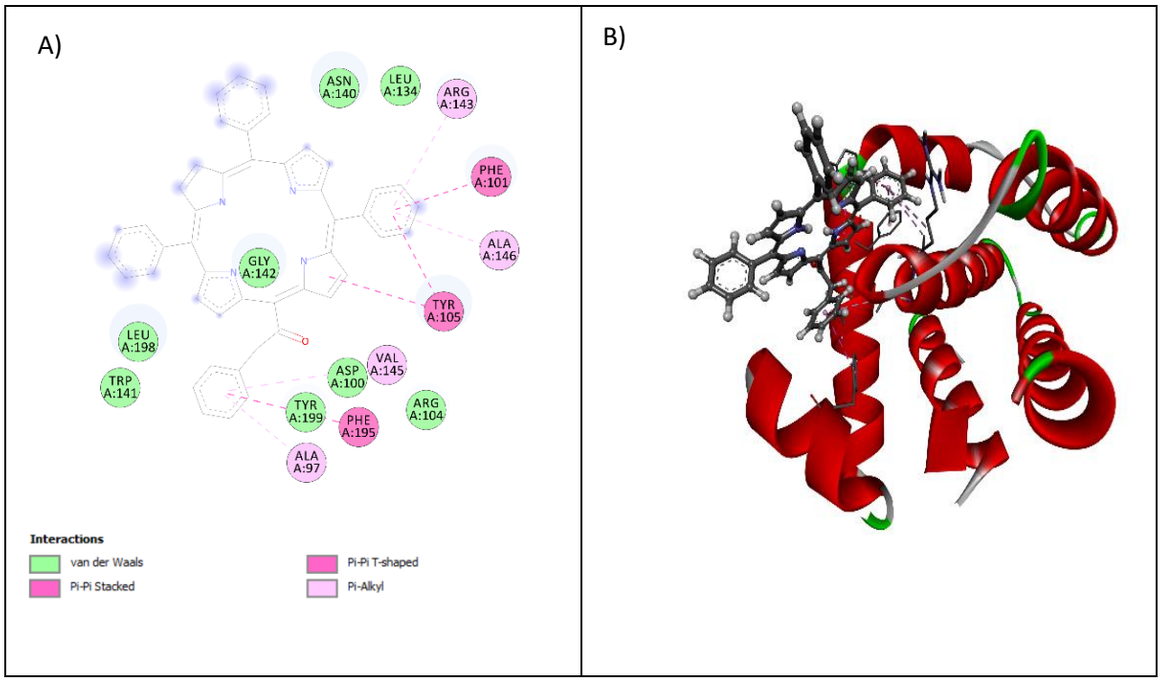

FIGURE 6. A) 2D orientation of the docked compound **15** in the active pocket of 4LVT.
B) 3D– Putative docking interaction of ligand **15** that was in complex of 4LVT

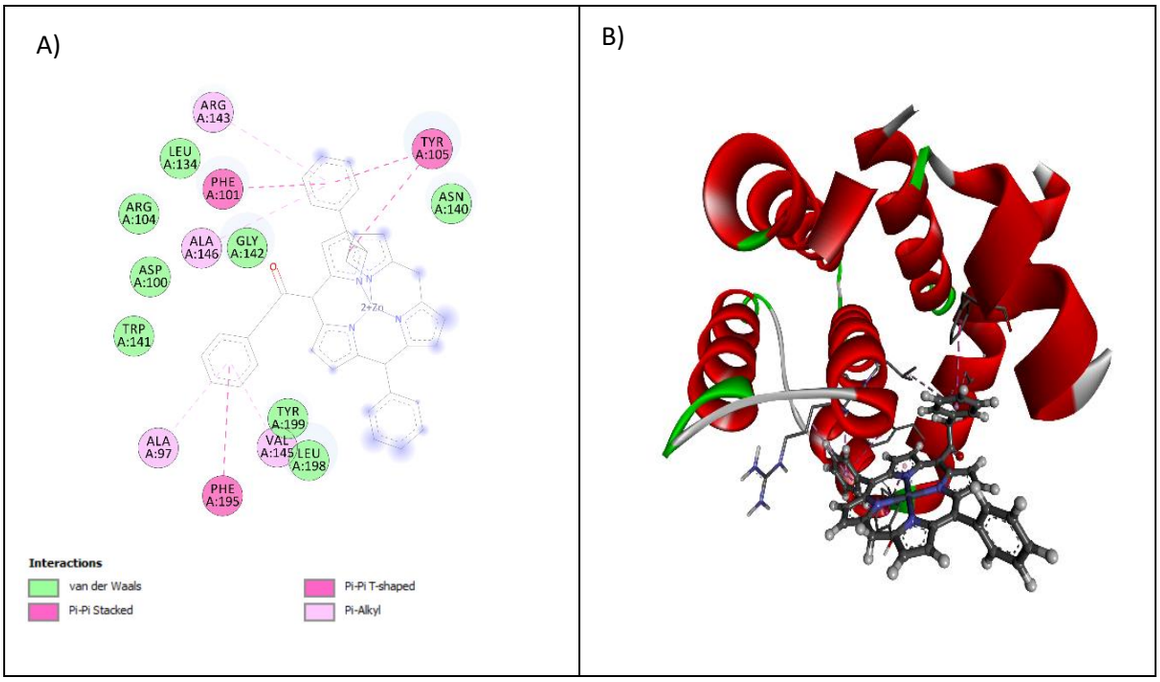

FIGURE 7. A) 2D orientation of the docked compound **20** in the active pocket of 4LVT.
B) 3D– Putative docking interaction of ligand **20** that was in complex of 4LVT

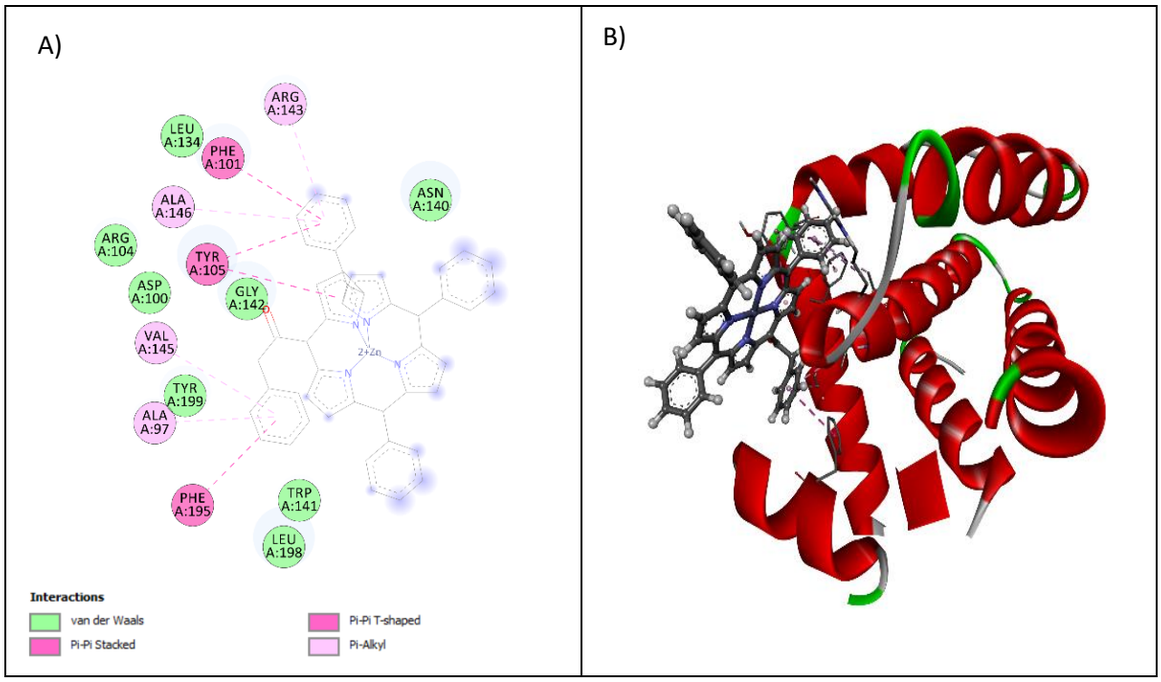

FIGURE 8. A) 2D orientation of the docked compound **21** in the active pocket of 4LVT.
B) 3D– Putative docking interaction of ligand **21** that was in complex of 4LVT

18	404	531, 569
19	406	538, 579

TABLE 2. Interaction types occurred between the compounds and 4LVT protein molecules

Compound	Hydrogen bond	Hydrophobic	Electrostatic
14	*	TYR105(5.386 Å) PHE101(4.975 Å) TYR105(4.783 Å) PHE195(4.956 Å) ALA97(4.735 Å) VAL145(5.344 Å) ARG143(5.423 Å) ALA146(4.703 Å)	**
15	*	TYR105(5.423 Å) PHE101(5.000 Å) TYR105(4.802 Å) PHE195(4.935 Å) ALA97(4.718 Å) VAL145(5.341 Å) ARG143(5.399 Å) ALA146(4.713 Å)	**
16	ASN140(2.997 Å)	TYR105(5.273 Å) PHE101(4.969 Å) PHE101(5.247 Å) TYR105(5.0247 Å) ARG143(5.423 Å) ALA146(4.505 Å) MET112(4.607 Å) ALA146(5.291 Å) ALA97(4.979 Å)	ARG143(4.976 Å)
17	ASN140(2.966 Å)	TYR105(5.245 Å) PHE101(4.916 Å) PHE101(5.230 Å) TYR105(5.050 Å) ARG143(5.468 Å) ALA146(4.444 Å) MET112(4.624 Å) ALA146(5.258 Å) ALA97(4.968 Å)	ARG143(4.771 Å)

18	ASN140(2.992 Å)	TYR105(5.248 Å) PHE101(4.892 Å) PHE101(5.227 Å) TYR105(5.023 Å) ARG143(5.461 Å) ALA146(4.438 Å) MET112(4.627 Å) ALA146(5.263 Å) ALA97(4.957 Å)	ARG143(4.844 Å)
19	ASN140(2.985 Å)	TYR105(5.231 Å) PHE101(4.911 Å) PHE101(5.219 Å) TYR105(5.046 Å) ARG143(5.475 Å) ALA146(4.443 Å) MET112(4.634 Å) ALA146(5.253 Å) ALA97(4.963 Å)	ARG143(4.759 Å)
20	*	TYR105(5.422 Å) PHE101(5.008 Å) TYR105(4.831 Å) PHE195(4.930 Å) ALA97(4.732 Å) VAL145(5.357 Å) ARG143(5.376 Å) ALA146(4.695 Å)	**
21	*	TYR105(5.463 Å) PHE101(5.035 Å) TYR105(4.795 Å) PHE195(4.901 Å) ALA97(4.741 Å) VAL145(5.369 Å) ARG143(5.403 Å) ALA146(4.753 Å)	**

*Compound had no aromatic hydrogen bond with the protein
**Compound had no electrostatic pi-cation

Molecular docking simulation analyses demonstrated that ligand-receptor of the four compounds **14-15** and **20-21** showed relatively low binding affinity. Interestingly, comparing the docking scores of metalated compounds shows greater or equal binding affinity scores compared to the free base structured compounds that is **20** and **21**. Bulkier compounds that is triphenyl substituted compounds (**17, 19, 15, 21**) gives lower binding affinity compared to diphenyl substituted compounds (**16, 18, 14, 20**). Ethynyl phenyl benzene substituted compounds **16** = **17** > **18** > **19** with hydrogen bond and electrostatic π-cation observed greater binding affinity.

Conclusion

In conclusion, meso-substituted porphyrin derivatives were efficiently synthesized with condensation, bromination and organolithium reactions. A solid violet shade of compounds of **10-13** via Sonogashira coupling technique and compounds **14-15 and 20-21** via Suzuki-Miyaura coupling were synthesized. These compounds with different bulkiness and lengths of linker conjugates have the potential to be linked with anticancer drugs to produce pro-drugs. Four distinct porphyrins and four metalloporphyrins were synthesized, manifesting discernible variations in peripheral substituents and core transition metal ions, as evident in their UV-VIS spectra. These porphyrin derivatives demonstrated an affinity for interacting with Bcl-2, with the interaction influenced significantly by electrostatic and van der Waals energies. Notably, porphyrins featuring less voluminous substituents exhibited a heightened propensity for binding with Bcl-2.

ACKNOWLEDGEMENT

This work was funded by grant FRGS/1/2019/STG01/UKM/02/18 from the Ministry of Higher Education. We thank the Universiti Kebangsaan Malaysia's Faculty of Science and Technology for providing the required laboratory space and technical support.

REFERENCES

Allouche, A. 2012. Software news and updates gabedit - A graphical user interface for computational chemistry softwares. *Journal of Computational Chemistry* 32: 174-182.

Bakar, M.A., Sergeeva, N.N., Juillard, T. & Senge, M.O. 2011. Synthesis of ferrocenyl porphyrins via suzuki coupling and their photophysical properties. *Organometallics* 30(11): 3225-3228.

Barillé-Nion, S., Lohard, S. & Juin, P.P. 2020. Targeting of bcl-2 family members during anticancer treatment: A necessary compromise between individual cell and ecosystemic responses? *Biomolecules* 10(8): 1-24.

Boscencu, R., Radulea, N., Manda, G., Machado, I.F., Socoteanu, R.P., Lupuliasa, D., Burloiu, A.M., Mihai, D.P. & Ferreira, L.F.V. 2023. Porphyrin macrocycles: General properties and theranostic potential. *Molecules* 28(3): 1149.

Dahms, K. & Senge, M.O. 2008. Triptycene as a rigid, 120° orienting, three-pronged, covalent scaffold for porphyrin arrays. *Tetrahedron Letters* 49(37): 5397-5399.

Eom, Y.H., Kim, H.S., Lee, A., Song, B.J. & Chae, B.J. 2016. BCL2 as a subtype-specific prognostic marker for breast cancer. *Journal of Breast Cancer* 19(3): 252-260.

Fathi, P. & Pan, Di. 2020. Current trends in pyrrole and porphyrin-derived nanoscale materials for biomedical applications. *Nanomedicine* 15(25): 2493-2515.

Feng, X. & Senge, M.O. 2001. An efficient synthesis of highly functionalized asymmetric porphyrins with organolithium reagents. *Journal of the Chemical Society. Perkin Transactions* 1(9): 1030-1038.

Gasteiger, J. & Marsili, M. 1980. Iterative partial equalization of orbital electronegativity-a rapid access to atomic charges. *Tetrahedron* 36(22): 3219-3228.

Giovannetti, R. 2012. The use of spectrophotometry UV-Vis for the study of porphyrins. In *Macro to Nano Spectroscopy,* edited by Uddin, J. InTech. doi:10.5772/2503

Gujarathi, P. 2020. Review on synthetic advances in porphyrins and metalloporphyrins. *International Journal of Chemical Studies* 8(3): 23-32.

Han, M. & Zhang, J.Z.H. 2010. Class I phospho-inositide-3-kinases (PI_3K_s) isoform-specific inhibition study by the combination of docking and molecular dynamics simulation. *Journal of Chemical Information and Modeling* 50(1): 136-145.

Hartnell, R.D., Edwards, A.J. & Arnold, D.P. 2002. Peripherally-metallated porphyrins: meso-η1-porphyrinyl-platinum(II) complexes of 5,15-diaryl- and 5,10,15- triarylporphyrins. *Journal of Porphyrins and Phthalocyanines* 6(11): 695-707.

Ion, R-M. 2017. Porphyrins and phthalocyanines: Photosensitizers and photocatalysts. In *Phthalocyanines and Some Current Applications,* edited by Yilmaz, Y. InTech. doi:10.5772/intechopen.68654

Kale, J., Osterlund, E.J. & Andrews, D.W. 2018. BCL-2 family proteins: Changing partners in the dance towards death. *Cell Death and Differentiation* 25(1): 65-80.

Locos, O.B. & Arnold, D.P. 2006. The Heck reaction for porphyrin functionalisation: Synthesis of meso-alkenyl monoporphyrins and palladium-catalysed formation of unprecedented meso-β ethene-linked diporphyrins. *Organic and Biomolecular Chemistry* 4(5): 902-916.

Marck, G., Villiger, A. & Buchecker, R. 1994. Aryl couplings with heterogeneous palladium catalysts. *Tetrahedron Letters* 33(20): 3277-3280.

Mohd Radzuan, N.H., Norazmi, N.A.Z., Ali, A.H., Abu Bakar, M., Agustar, H.K., Mohd Abd Razak, M.R. & Hassan, N.I. 2021. Sintesis, aktiviti antiplasmodium dan kesitotoksikan secara *in vitro* sebatian porfirin logam ke atas strain *Plasmodium falciparum* K1. *Sains Malaysiana* 50(10): 2945-2956.

Mohjer, F., Mofatehnia, P., Rangraz, Y. & Heravi, M.M. 2021. Pd-free, Sonogashira cross-coupling reaction. An update. *Journal of Organometallic Chemistry* 936: 121712.

Monvall, E. 1976. Statsbudgeten: de stora reformerna gäller arbetslivet. *Tidskrift for Sveriges sjukskoterskor* 43(2): 54-58.

Morris, J.L., Gillet, G., Prudent, J. & Popgeorgiev, N. 2021. Bcl-2 family of proteins in the control of mitochondrial calcium signalling: An old chap with new roles. *International Journal of Molecular Sciences* 22(7): 3730.

Nakano, A., Yasuda, Y., Yamazaki, T., Akimoto, S., Yamazaki, I., Miyasaka, H., Itaya, A., Murakami, M. & Osuka, A. 2001. Intramolecular energy transfer in S1- and S2-states of porphyrin trimers. *Journal of Physical Chemistry A* 105(20): 4822-4833.

Nowak-Krol, A., Plamont, R., Canard, G., Edzang, J.A., Gryko, T., Balaban, T.S., Nowak-krol, A., Plamont, R., Canard, G., Edzang, J.A., Gryko, D.T., Nowak-król, A., Plamont, R., Canard, G. & Edzang, A. 2020. An efficient synthesis of porphyrins with different meso substituents that avoids scrambling in aqueous media. *Chemistry* 21(4): 1488-1498.

Park, J.M., Hong, K.I., Lee, H. & Jang, W.D. 2021. Bioinspired applications of porphyrin derivatives. *Accounts of Chemical Research* 54(9): 2249-2260.

Pathak, P., Zarandi, M.A., Zhou, X. & Jayawickramarajah, J. 2021. Synthesis and applications of porphyrin-biomacromolecule conjugates. *Frontiers in Chemistry* 9(November): 1-30.

Phan, A.T., Kuryavyi, V., Gaw, H.Y. & Patel, D.J. 2005. Small-molecule interaction with a five-guanine-tract g-quadruplex structure from the human *MYC* promoter. *Nature Chemical Biology* 1(3): 167-173.

Radzuan, N.H.M., Malek, N.H.A., Ngatiman, M.F., Xin, T.K., Bakar, M.B., Hassan, N.I. & Bakar, M.A. 2018. Synthesis and X-ray single crystal study of 5-(4,4,5,5 – tetramethyl – 1,3,2 – dioxoborolane) – 10,20 – diphenylporphyrin. *Sains Malaysiana* 47(9): 2083-2090.

Rathi, P.C., Ludlow, R.F. & Verdonk, M.L. 2020. Practical high-quality electrostatic potential surfaces for drug discovery using a graph-convolutional deep neural network. *Journal of Medicinal Chemistry* 63(16): 8778-8790.

Ryan, A., Gehrold, A., Perusitti, R., Pintea, M., Fazekas, M., Locos, O.B., Blaikie, F. & Senge, M.O. 2011. Porphyrin dimers and arrays. *European Journal of Organic Chemistry* 29: 5817-5844.

Saini, G., Dalal, V., Savita, B.K., Sharma, N., Kumar, P. & Sharma, A.K. 2019. Molecular docking and dynamic approach to virtual screen inhibitors against Esbp of *Candidatus* Liberibacter asiaticus. *Journal of Molecular Graphics and Modelling* 92: 329-340.

Senge, M.O. & Feng, X. 2000. Regioselective reaction of 5,15-disubstituted porphyrins with organolithium reagents - Synthetic access to 5,10,15-trisubstituted porphyrins and directly meso-meso-linked bisporphyrins. *Journal of the Chemical Society, Perkin Transactions* 1(21): 3615-3621.

Shanmugathasan, S., Johnson, C.K., Edwards, C., Matthews, E.K., Dolphin, D. & Boyle, R.W. 2000. Regioselective halogenation and palladium-catalysed couplings on 5,15-diphenylporphyrin. *Journal of Porphyrins and Phthalocyanines* 4(3): 228-232.

Van Der Spoel, D., Lindahl, E., Hess, B., Groenhof, G., Mark, A.E. & Berendsen, H.J.C. 2005. GROMACS: Fast, flexible, and free. *Journal of Computational Chemistry* 26(16): 1701-1718.

Varnado Jr., C.D. & Bielawski, C.W. 2012. 5.08 - Condensation polymers via metal-Catalyzed coupling reactions. *Polymer Science: A Comprehensive Reference* 5: 175-194.

Yin, L. & Liebscher, J. 2007. Carbon-carbon coupling reactions catalyzed by heterogeneous palladium catalysts. *Chemical Reviews* 107(1): 133-173.

Zheng, W., Shan, N., Yu, L. & Wang, X. 2008. UV-visible, fluorescence and EPR properties of porphyrins and metalloporphyrins. *Dyes and Pigments* 77(1): 153-157.

*Corresponding author; email: muntaz@ukm.edu.my